Modeling of Dendritic Structure Evolution During Solidification of Al-Cu Alloy

A. Zyska *, K. Boroń, P. Kordas
Foundry Department, Czestochowa University of Technology,
Al. Armii Krajowej 19, 42-200 Częstochowa, Poland
* Corresponding author: E-mail address: zyska@wip.pcz.pl

Abstract

The paper presents the cellular automaton (CA) model for tracking the development of dendritic structure in non-equilibrium solidification conditions of binary alloy. Thermal, diffusion and surface phenomena have been included in the mathematical description of solidification. The methodology for calculating growth velocity of the liquid-solid interface based on solute balance, considering the distribution of the alloy component in the neighborhood of moving interface has been proposed. The influence of solidification front curvature on the equilibrium temperature was determined by applying the Gibbs Thomson approach. Solute and heat transfer equations were solved using the finite difference method assuming periodic boundary conditions and Newton cooling boundary condition at the edges of the system. The solutal field in the calculation domain was obtained separately for solid and liquid phase. Numerical simulations were carried out for the Al-4 wt.% Cu alloy at two cooling rates 15 K/s and 50 K/s. Microstructure images generated on the basis of calculations were compared with actual structures of castings. It was found that the results of the calculations are agreement in qualitative terms with the results of experimental research. The developed model can reproduce many morphological features of the dendritic structure and in particular: generating dendritic front and primary arms, creating, extension and coarsening of secondary branches, interface inhibition, branch fusion, considering the coupled motion and growth interaction of crystals.

Keywords: Solidification, Cellular automata, AlCu alloys, Structure modeling

1. Introduction

The structure of the casting formed in the solidification process is the main factor influencing its final functional properties. The mechanical properties of castings as well as their tendency to hot cracking change depending on the grain size, the secondary dendrite arm spacing and the degree of microsegregation. In this context, the solidification is a complex process and its mathematical description requires taking into account a number of physical phenomena.

The growth of dendritic structures during solidification can be analyzed based on experimental studies, analytical models and numerical models [1-4]. The analytical models developed in the last century were focused on the mathematical description of the

dendrite tip movement and the determination of the relationship between its velocity and melt undercooling. Current numerical models can realistically simulate dendritic growth on a micro scale, reproducing many morphological features such as: curvature of the dendrite tip, the length of incubation before the generation of second-order arms, the dendrites arms spacing and the shape and size of the branches [4-9].

Two numerical techniques, (PF) Phase Field method and (CA) Cellular Automaton are most often proposed to the modeling of microstructure [10, 11]. They are applied to the simulation of dendritic development in the solidification process considering the growth of columnar and equiaxed crystals. The CA models are based on equations developed in the classical theory of solidification of metal alloys. The reproduction of structural morphology is performed by calculating the momentary position

of the solidification front in cells with a length of 10^{-6} m. The algorithms solve simultaneously the heat and solute transfer equations, and sometimes convective diffusion equation in the entire domain. In the interface cells, the front curvature, its anisotropy, surface tension and local equilibrium are computed in a coupled manner. Various nucleation methods in the initial solidification period can also be considered. The mathematical description of these physical phenomena in CA models allows the reproduction of many structural features corresponding to realistic solidification conditions. During solidification simulation can to observe the subsequent stages of dendrite growth, multi-dendritic interactions, as well as the formation and development of eutectic grains. Furthermore, based on the concentration fields obtained from the modeling, it is possible to determine the degree of solute segregation at the different cooling rates of the castings [5-14].

The CA method is applied to trace the evolution of equiaxed and columnar dendrites and the globular structures in the two- and three-dimensional space [5-12]. This technique is also used to simulate dendritic growth in the presence of liquid metal convection and the coupled phase growth of regular and irregular eutectics [13-15].

2. Model description

In the present model, a two-dimensional square automaton divided into uniform cells with length Δx is considered. Employing the spatial indices i and j and the time index t, each cell is described by the following quantities: temperature – $T(i,j,t)$, concentration of the solute – $C(i,j,t)$, fraction of the solid phase – $f_s(i,j,t)$, phase state – $P(i,j,t)$, interfacial curvature - κ (i,j,t), preferential crystallographic orientation angle – $\theta_0(i,j,t)$. During solidification, cells change their state from liquid ($f_S = 0$) to interface ($0 < f_S < 1$) and then to solid ($f_S = 1$).

In the computational procedure, the Moore and von Neumann neighbourhoods was applied. The first of them was adopted to solve the heat and solute transport equations, while the second one was used to calculate the quantities describing interfacial phenomena. In order to limit the artificial anisotropy of dendrite growth induced by the square lattice of cellular automaton, the procedure of capturing the liquid cells to the interface based on the momentary location of the solidification front was used [7]. The calculations were started by randomly determining the position of the nucleation cells and assigning them also a randomly preferential crystallographic orientation [5, 8, 10,12]. The initial temperature T_0 and solute concentration C_0 in the entire domain was homogeneous. Further evolution of the structure is controlled by the solute diffusion in the solid and liquid phase, heat transfer and increment of the solid fraction expressed by the system of model equations.

The temperature field in the calculation domain was obtained by solving the 2D heat transport equation by the finite difference method:

$$\frac{\partial T(x,y,t)}{\partial t} = a_T \left(\frac{\partial T^2(x,y,t)}{\partial^2 x} + \frac{\partial T^2(x,y,t)}{\partial^2 y} \right) + \frac{L}{\rho c_p} \frac{\partial f_S}{\partial t} \quad (1)$$

where: T – temperature, t - time, a_T – heat diffusivity, c_p – specific heat, f_S – solid fraction ρ - density and L – latent heat of solidification.

Cooling of the domain at the walls is determined by:

$$-\lambda \frac{\partial T}{\partial n} = h(T - T_\infty) \quad (2)$$

where: n - the normal vector to the wall, λ – thermal conductivity, h – the heat transfer coefficient, T_∞ – external temperature

The solute conservation equation was solved independently for solid and liquid phase applying finite differences method:

$$\frac{\partial C_I(x,y,t)}{\partial t} = D_I \left(\frac{\partial^2 C_I(x,y,t)}{\partial x^2} + \frac{\partial^2 C_I(x,y,t)}{\partial y^2} \right) \quad (3)$$

where: C_I – solute concentration, D_I – the diffusion coefficient, $C_I = C_s$ and $D_I = D_S$ for solid or $C_I = C_L$ and $D_I = D_L$ for liquid phase, the interface cells are treated as a liquid phase.

Equation [3] is solved considering local equilibrium composition, solute partition coefficient and solute balance at the moving interface:

$$C_L^F = C_0 + \frac{1}{m_L}[T^F - T_L + \Gamma \kappa f(\varphi, \theta_0)] \quad (4)$$

$$k_0 = \frac{C_S^F}{C_L^F} \quad (5)$$

$$v_n C_L^F (1 - k_0) = \left[-D_L \left(\frac{\partial C_L}{\partial x} + \frac{\partial C_L}{\partial y} \right) + D_S \left(\frac{\partial C_S}{\partial x} + \frac{\partial C_S}{\partial y} \right) \right] \cdot n \quad (6)$$

where: C_0 – initial concentration of solute, T^F – temperature at the interface, T_L – liquidus temperature, Γ – Gibbs-Thomson coefficient m_L – the slope of the liquidus, κ – interfacial curvature, $f(\varphi, \theta_0)$ is a function describing the anisotropy of the surface tension, C_L^F and C_S^F are the equilibrium liquid and solid concentrations at the interface, v_n – the normal velocity of moving front, n – the unit normal vector.

The SL interface curvature induces capillary effects which alter the liquidus temperature and cause curvature undercooling. In addition, the solidification front curvature influences the evolution of the dendrite tip. The local interfacial curvature κ and the anisotropy function $f(\varphi, \theta_0)$ in Eq. [4] are calculated using the following equations:

$$\kappa = \frac{1}{a} \left[1 - 2 \frac{f_S + \sum_{k=1}^N f_S(k)}{N+1} \right] \quad (7)$$

$$f(\varphi, \theta_0) = (1 - \delta \cos[m_S(\varphi - \theta_0)]) \quad (8)$$

$$\varphi = arctan\left[\frac{\partial f_S}{\partial x} \cdot \left(\frac{\partial f_S}{\partial y}\right)^{-1}\right] \tag{9}$$

where: N – the total number of neighboring cells, m_s – crystal-order parameter, for cubic symmetry $m_s = 4$, δ – the anisotropy coefficient, θ_0 – crystallographic orientation angle, φ – normal to the moving interface (the growth direction).

The values of the interface velocities for interface cells are computed based on equations (4), (5) and (6). For v_x the finite difference formula takes the form:

$$
\begin{aligned}
v_y(i,j) = \frac{D_L}{a(1-k_0)}&\left[\left(1 - \frac{C_L(i,j-1)}{C_L^F(i,j)}\right)\Phi_1[f_S(i,j), f_S(i,j-1)]\right.\\
&\left. + \left(1 - \frac{C_L(i,j+1)}{C_L^F(i,j)}\right)\Phi_1[f_S(i,j), f_S(i,j+1)]\right]\\
+ \frac{k_0 D_S}{a(1-k_0)}&\left[\left(1 - \frac{C_S(i,j-1)}{C_S^F(i,j)}\right)\Phi_2[f_S(i,j), f_S(i,j-1)]\right.\\
&\left. + \left(1 - \frac{C_S(i,j+1)}{C_S^F(i,j)}\right)\Phi_2[f_S(i,j), f_S(i,j+1)]\right] \tag{10}
\end{aligned}
$$

where the functions $\Phi_1[f_1, f_2]$ and $\Phi_2[f_1, f_2]$ are adapted to determine the presence of the concentration gradients on both sides of the moving interface. They return a number of 1 if $0 < f_1 < 1$ and $f_2 < 1$ for function Φ_1, and if $0 < f_1 < 1$ and $f_2 = 1$ for function Φ_2. Else, the returned number is 0. The differentiation in the x-direction is analogous. The local equilibrium concentration at the solidification front, C_L^F, is computed from Eq. [4], in which the temperature T^F is obtained by solving Eq. [5]. Knowing the velocity components, the increment of solid fraction in one time step, δt, is obtained from [6]:

$$\delta f_S = \frac{\delta t}{a}\left(v_x + v_y - v_x v_y \frac{\delta t}{a}\right) \tag{11}$$
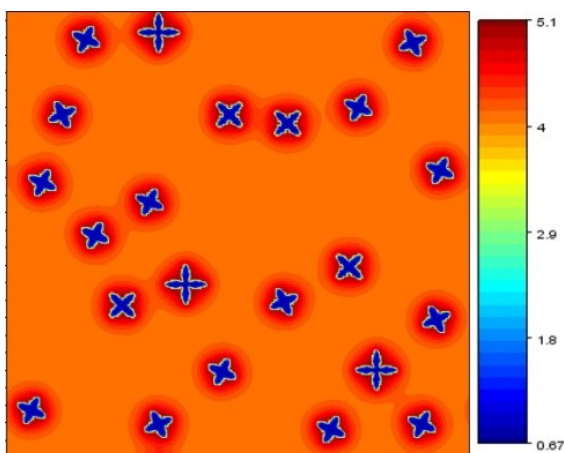
3. Simulation results

Modelling of dendritic growth was carried out for the Al - 4%wt. Cu alloy. The thermophysical properties used in simulations can be found in Ref. [5]. Computing was carried out in the domain of 304x304 unit cells with the length of one cell was 2 mm. Newton cooling boundary conditions were applied at all walls of the model. The average cooling rate in the computing domain was 50K/s (in the absence of internal heat sources). Cu concentration fields were obtained by solving the solute transfer equation with periodic conditions. Calculation was started assuming a domain temperature equal to liquidus temperature. The stages of dendrite development and the distribution of solute in solid, interface and liquid during solidification is presented in the Fig. 1. Copper concentrations in interfacial cells are average concentrations resulting from the mass balance. During morphological evolution, such dendritic features as generating solidification front and primary arms, creating and coarsening of secondary branches, interface inhibition, branch fusion and the coupled motion and growth interaction of crystals is observed.

In the initial period, the main dendrite arms grow relatively uniformly along the preferential directions defined by the θ_0 angles. The further course of solidification depends strongly on the interaction of concentration fields around dendrites causing significant changes in the shape of dendrites and their growth rate.

The location of nuclei, crystallographic orientation and coupled motion determine the morphology of individual dendrites. The large distance between the nucleation cells and the orientation ensuring a long time of free growth result in the formation of large primary branches of dendrites. The interface inhibition by the neighboring dendrite tips leads to the development of secondary branches and to the coarsening of the primary arms.
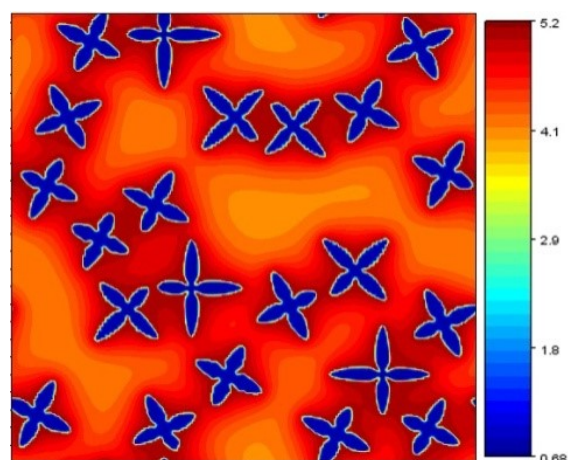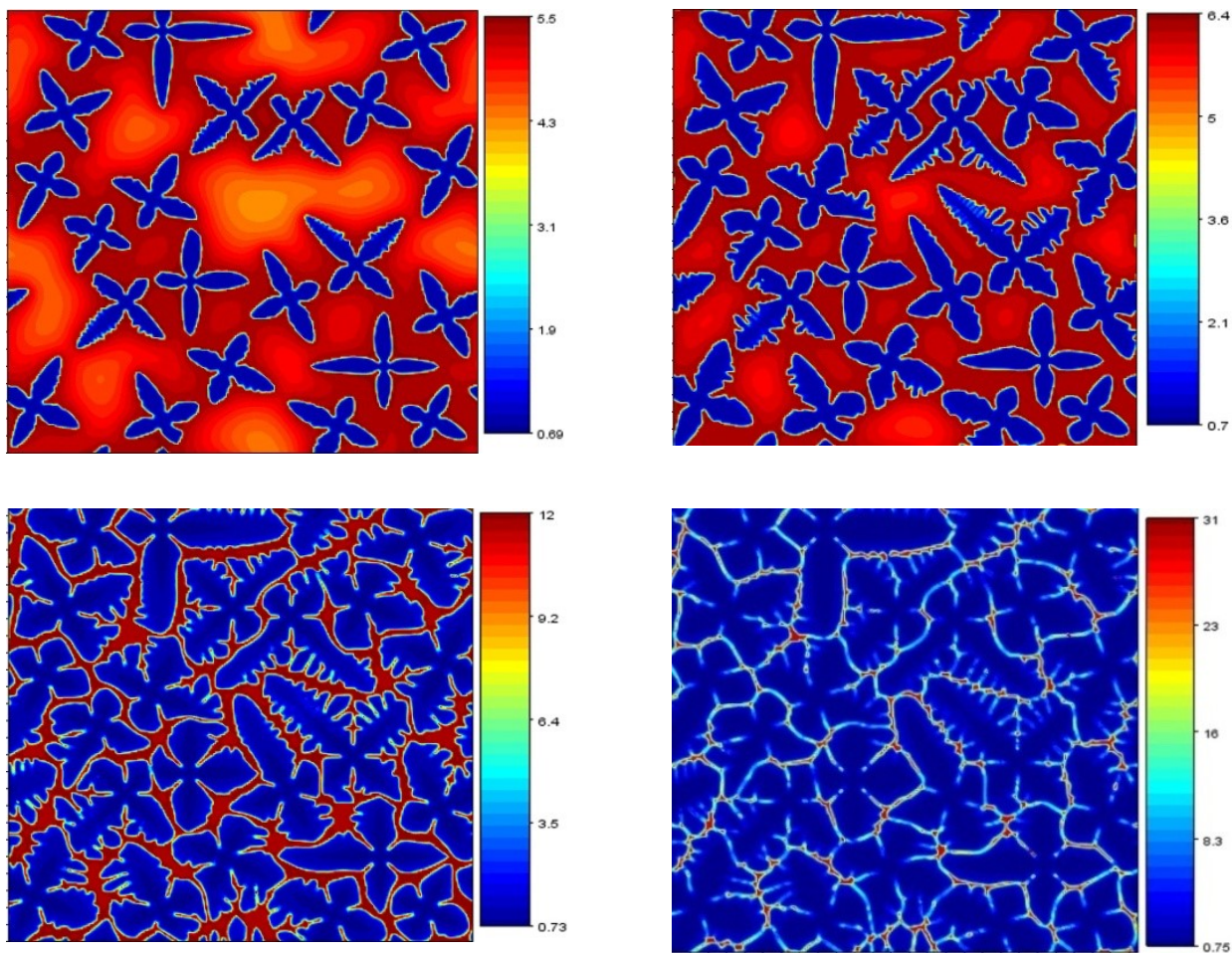
Fig. 1. Simulated dendritic evolution and solute fields during solidification of Al+4 wt% Cu alloy with the cooling rate of 50K/s

The size and shape of the secondary branches depend on the interaction of copper concentration fields. The possibility of moving the dendritic front to the zones of low Cu concentration promotes the extension of secondary arms. Interface inhibition and branch fusion proceed strongly at the final stage of the process. Dendrites are surrounded by small liquid layers with high concentration of solute. The liquid phase composition contains about 30% Cu (the last concentration map in Figure 1).

Figures 2a and 3a show actual structure of Al-4 % wt. Cu casts using sand and metal molds, respectively. The corresponding final images of structure obtained from the numerical simulation, assuming the average cooling rate 15 K/s and 50 K/s are presented in Figs 2b and 3b. It can be seen that the modeled grain shapes and grain sizes are in very close resemblance to experimental micrographs. The grain size and the dendrite arm spacing in the die casting is significantly smaller than in the sand casting, due to greater heat dissipation and the higher nucleation density.
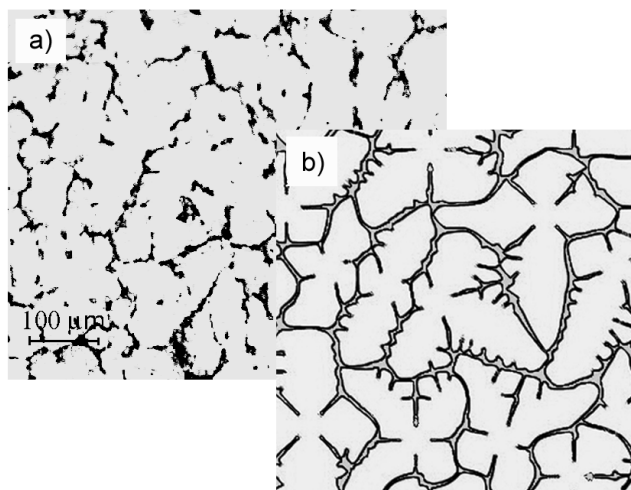

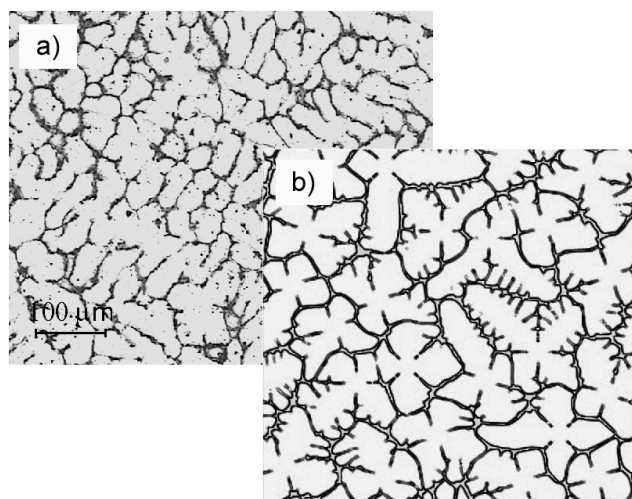Fig. 2. Structure of Al+4% wt. Cu alloy: a) actual in the sand casting, b) modelled – 15 K/s

Fig. 3. Structure of Al+4% wt. Cu alloy: a) actual in the die casting, b) modelled – 50 K/s

In order to determine the agreement numerical results with experimental results was carried out measurements of the spacing of secondary arms (SDAS). Measurements were made for actual structures and for structures generated from the model in the final phase of solidification. The average values of secondary dendrite arm spacing for various local solidification times are shown in Figure 4. The figure also shows the results of SDAS from the literature. The presented comparison shows that the results of numerical simulations correspond well with the experiment and with values reported in the literature.
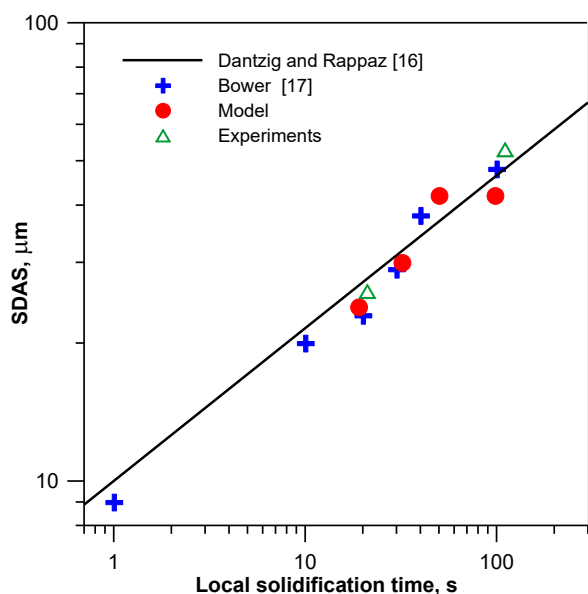

Fig. 4. Comparison of calculated SDAS with experimental and literature results

4. Conclusions

A dendritic evolution model in castings of aluminium-copper alloys was developed using a cellular automaton method. Thermal, diffusion and surface phenomena have been included in the mathematical description of solidification. Numeric simulations can reproduce many morphological features of the dendritic structure, such as: generating dendritic front and primary arms, creating, extension and coarsening of secondary branches, interface inhibition, fusion of branches, considering the coupled motion and growth interaction of crystals. The generated structures of alloy based on numerical simulations and calculated SDAS values for various local solidification times are agreement with experimental results and literature data. The developed CA model can be applied to predict the AlCu alloy structure in a quantitative and qualitative manner.

References

[1] Miller, J.D., Yuan, L., Lee, P.D. & Pollock T.M. (2014). Simulation of diffusion-limited lateral growth of dendrites during solidification via liquid metal cooling. *Acta Materialia*. 69, 47-59.

[2] Genau, A.L., Freedman, A.C. & Ratke, L. (2013). Effect of solidification conditions on fractal dimension of dendrites. *Journal of Crystal Growth*. 363, 49-54.

[3] Stefanescu, D.M. (2009). *Science and Engineering of Casting Solidification*. Springer.

[4] Wołczyński, W., Ivanova, A.A., Kwapisiński, P. & Olejnik, E. (2017). Structural Transformations Versus Hard Particles Motion in the Brass Ingots. *Archives of Metallurgy and Materials*. 62(4), 2461-2467.

[5] Beltran-Sanchez, L. & Stefanescu, D.M. (2004). A Quantitative Dendrite Growth Model and Analysis of Stability Concepts. *Metallurgical and Materials Transactions A*. 35, 2471-2485.

[6] Kuangfei, W., Shan, L., Guofa, M., Changyun, L., Hengzhi, F. (2010). Simulation of microstructural evolution in directional solidification of Ti-45at.%Al alloy using cellular automaton method. *China Foundry*. 7, 47-51.

[7] Zyska, A., Konopka, Z., Łągiewka, M. & Nadolski, M. (2016). Modelling of the dendritic crystallization by the cellular automaton method. *Archives of Foundry Engineering*. 16(1), 99-106.

[8] Zhu, M.F., Cao, W., Chen, S.L., Hong, C.P. & Chang, Y.A. (2007). Modeling of Microstructure and Microsegregation in Solidification of Multi-Component Alloys. *Journal of Phase Equilibria and Diffusion*. 28, 130-138.

[9] Zhu, M.F., Kim, J.M. & Hong, C.P. (2001). Modeling of Globular and Dendritic Structure Evolution in Solidification of an Al–7%Si Alloy. *ISIJ International*. 41(9), 992-998.

[10] Zaeem, M.A., Yin, H. & Felicelli, S.D. (2013). Modeling dendritic solidification of Al–3%Cu using cellular automaton and phase-field methods. *Applied Mathematical Modelling*. 37, 3495-3503.

[11] Choudhury, A., Reuther, K., Wesner, E. & Rettenmayr, M. (2012). Comparison of phase-field and cellular automaton

models for dendritic solidification in Al–Cu alloy. *Computational Materials Science*. 55, 263-268.

[12] Beltran-Sanchez, L. & Stefanescu, D.M. (2003). Growth of Solutal Dendrites: A Cellular Automaton Model and Its Quantitative Capabilities. *Metallurgical and Materials Transactions A. 34*, 367-382.

[13] Luo, S., Wang, W. & Zhu, M. (2018). Cellular automaton modeling of dendritic growth of Fe-C binary alloy with thermosolutal convection. *International Journal of Heat and Mass Transfer*. 116, 940-950.

[14] Chen, R., Xu, Q. & Liu, B. (2016). Modeling of aluminum-silicon irregular eutectic growth by cellular automaton model. *China Foundry*. 13(2), 114-122.

[15] Xiong, S. & Wu, M. (2012). Experimental and Modeling Studies of the Lamellar Eutectic Growth of Mg-Al Alloy *Metallurgical and Materials Transactions A*. 43, 208-218.

[16] Dantzig, J.A., Rappaz, N. (2016). *Solidification*. Engineering Science, Epfl Press.

[17] Bower, T.F., Brody, H.D. & Flemings, M.C. (1996). Measurements of solute redistribution in dendritic solidification. *Transaction of Metallurgical Society of AIME*, 236, 624-634.